Korean Chem. Eng. Res., 61(3), 463-471 (2023)
https://doi.org/10.9713/kcer.2023.61.3.463
PISSN 0304-128X, EISSN 2233-9558

Green Synthesis of Dual Emission Nitrogen-Rich Carbon Dot and Its Use in Ag^+ Ion and EDTA Sensing

Le Thuy Hoa, Jin Suk Chung and Seung Hyun Hur†

School of Chemical Engineering, University of Ulsan, 93 Daehak-ro, Nam-gu, Ulsan, 44610, Korea
(Received 27 June 2023; Received in revised from 30 June 2023; Accepted 30 June 2023)

Abstract – Nitrogen-rich carbon dots (NDots) were synthesized by using uric acid as carbon and nitrogen sources. The as-synthesized NDots showed strong dual emissions at 420 nm and 510 nm with excitation at 350 nm and 460 nm, respectively. The physicochemical analyses such as X-ray photoelectron spectroscopy, Transmission electron microscopy and Fourier transform infrared spectroscopy were used to analyze the chemical, physical and morphological structures of NDots. The as-synthesized NDots exhibited wide linear range (0-100 μM) and very low detection limit (124 nM) in Ag^+ ion sensing. In addition, Ag^+ saturated NDots could be used as an EDTA sensor by the EDTA induced PL recovery.

Key words: Carbon dots, Dual emission, Quenching, Silver ion, EDTA, Sensor

1. Introduction

Carbon-based materials such as carbon nanotube, fullerene, graphene or graphene oxide (GO) have been widely studied due to their unique properties according to the various morphologies and structures [1,2]. As a new member of carbon nanomaterials, fluorescent carbon dots (CDs) have attracted increasing attention in the fields of chemistry, physics, materials, etc. Due to their unique optical, electrical properties and ecofriendly feature, CDs are considered as one of the most promising materials in many application areas, including optoelectronic devices [3,4], catalysts [5,6], biosensors [7,8], and bio-imaging [9,10]. Generally, the common carbon sources to create the CDs are sodium citrate [11,12], glucose [13], graphene oxide [14,15], citric acid [16,17] or natural bio-sources like milk [18], fruit juice [19,20], hair fiber [21], konjac [22], coffee [23], and the PL phenomena of various CDs are totally different according to their sources. Recently, adjusting their compositions and structures by doping of CDs with other non-metallic elements such as nitrogen [18,22], sulfur [21,24], boron [25,26], etc. to endow specific properties to CDs, has been tried extensively. In particular, a dopant dopant such as nitrogen can inject electrons into carbon-based material and thus the electronic properties and local chemical reactivity of CDs can be highly enhanced. Based on previous studies, the nitrogen doped CDs were synthesized by using different nitrogen sources such as aqueous ammonia [27], amino acids [28], ammonium citrate [29] or milk [18], combined with other chemicals to make CDs emit various colors including blue, green, and red. However, these processes are complicated, time-consuming, toxic, or the resulting CDs exhibit low quantum yield, which makes them difficult to use in practical applications.

In this work, we prepared highly photoluminescent nitrogen-rich CDs (NDots) from uric acid which can act as a nontoxic carbon and nitrogen source by a large scalable hydrothermal synthesis. The as-synthesized NDots showed a strong dual fluorescence with a high quantum yield of 69% of blue emission and 61% of green emission. When they were used as a fluorescent probe for the detection of silver ion, they exhibited a wide linear range and very low detection limit. In addition, they also could be used as highly sensitive EDTA sensor by the recovered PL after EDTA addition to the Ag^+ saturated NDots.

2. Experimental

2-1. Reagents

Uric acid ($C_5H_4N_4O_3$, ≥ 99%), quinine hemisulfate salt monohydrate ($C_{20}H_{24}N_2O_2 \cdot 0.5H_2O_4S \cdot H_2O$, ≥ 98.0%), fluorescein sodium salt ($C_{20}H_{10}Na_2O_5$, ≥ 95.0%), L-cysteine (L-cys), glutaric acid (GA), glutamic acid (GtamA) and dopamine (DP) were purchased from Sigma–Aldrich Co. (USA). All the metal ion precursors such as $AgNO_3$, $CaCl_2$, $CoCl_2 \cdot 6H_2O$, $CuCl_2 \cdot 2H_2O$, $FeSO_4 \cdot 7H_2O$, $FeCl_3 \cdot 6H_2O$, KCl, LiCl, $MgCl_2 \cdot 6H_2O$, $Mn(CH_3COO)_2 \cdot 4H_2O$, NaCl, $NiCl_2 \cdot 6H_2O$, $Pb(NO_3)_2$, $SnCl_2 \cdot 2H_2O$, $ZnCl_2$ were obtained from Daejung Chemical Co. (Korea) and metal ion solutions were prepared in deionized water from the respective salts. Glycine (Gly), ascorbic acid (AA), citric acid (CA), glucose (GC), sucrose (Suc), maltose (Mal) and ethylenediaminetetraacetic acid (EDTA) were also purchased from Daejung Chemical Co. (Korea). All the chemicals were used as received without further purification.

† To whom correspondence should be addressed.
E-mail: shhur@ulsan.ac.kr

2-2. Synthesis of NDots

The NDots were prepared by hydrothermal process. 100 mg of uric acid was dissolved in 20 ml distilled (DI) water and sonicated for 30 min. Then, the solution was transferred to a Teflon-lined autoclave with a stainless-steel shell. The autoclave was kept at 180 ℃ for 5 h and cooled room temperature slowly. The resulting solution was washed with ethanol and centrifuged at 9,000 rpm for 30 min. Finally, the NDots were collected and re-dispersed into DI water.

2-3. Instrument analysis

The chemical and physical structures of the NDots were investigated using transmission electron microscopy (TEM, JEOL JEM-2100F, USA). X-ray photoelectron spectra were obtained using a X-ray photoelectron spectroscope (XPS, K-Alpha, Thermo Fisher Scientific ESCALAB 250Xi, USA) with an Al Kα X-ray source (1486.6 eV) and the UV-Vis spectra were recorded using double-beam UV-Vis spectrophotometer (Analytik Jena, Specord 210 Plus, German). Fourier transform infrared spectroscopy (FTIR) study was conducted with a Nicolet iS5 instrument (Nicolet Instrument, Thermo Company, USA). Fluorescence excitation and emission spectra were collected with a Cary Eclipse fluorescence spectrophotometer (Agilent Technologies, USA).

2-4. Quantum yield measurement

Due to the dual emission properties of NDots, the quantum yield of NDots was calculated using two standard references of quinine hemisulfate salt monohydrate (dissolved in 0.1 M H_2SO_4, excited at 350 nm, QY = 0.54) [30] and fluorescein sodium salt (dissolved in 0.01 M NaOH, excited at 460 nm, QY = 0.92) [31] according to the following equation:

$$Q_{dot} = Q_{st}\frac{I_{dot}}{I_{st}}\frac{OD_{st}}{OD_{dot}}\left(\frac{\eta_{dot}}{\eta_{st}}\right)^2 \quad (1)$$

where the subscripts "*dot*" and "*st*" refer to the NDots samples and the standard reference fluorophore, respectively; Q is the quantum yield; I is the integrated intensity, OD is the optical density of the samples at the excitation wavelength, and η is refractive index of the solutions.

2-5. Spectrofluorimetric measurements

0.3 mL of NDots (50 μg/mL) was diluted by 2.5 mL DI water and then an appropriate volume of Ag^+ solution was added. The fluorescence was measured in a quartz cuvette at 430 nm and 520 nm with excitation at 350 nm and 460 nm, respectively. All the experiments were performed at room temperature. The selectivity for Ag^+ ion was confirmed by adding other metal ion solutions instead of Ag^+ ions in a similar way.

2-6. Detection of Ag^+ ion in real sample

The sensing performance of NDots for real sample was examined by tap water that was collected from the lake in our city. The lake samples were filtered and centrifuged for 30 minutes to remove the all visible residuals before use.

3. Results and Discussion

3-1. Characterization of NDots

The NDots fabrication process is illustrated in Fig. 1a. A transparent bright green solution is obtained after hydrothermal

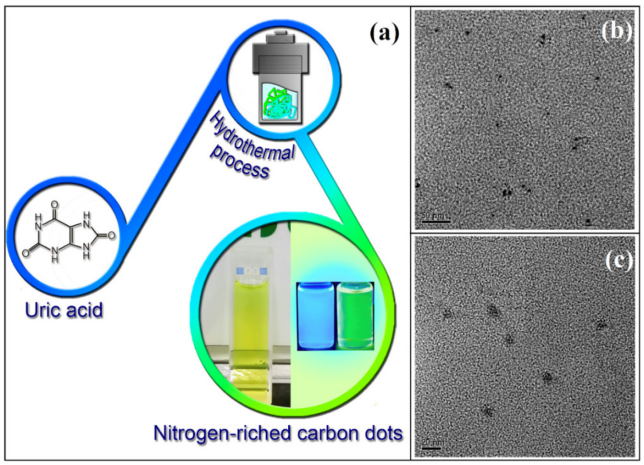

Fig. 1. (a) The schematic representation of the NDots preparation. (b, c) the TEM image of NDots.

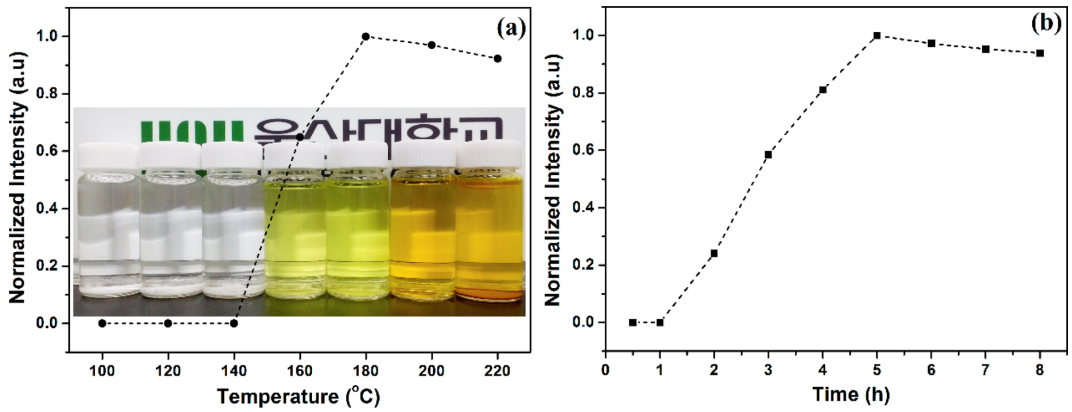

Fig. 2. Normalized PL intensity of NDots according to (a) reaction temperature and (b) reaction time.

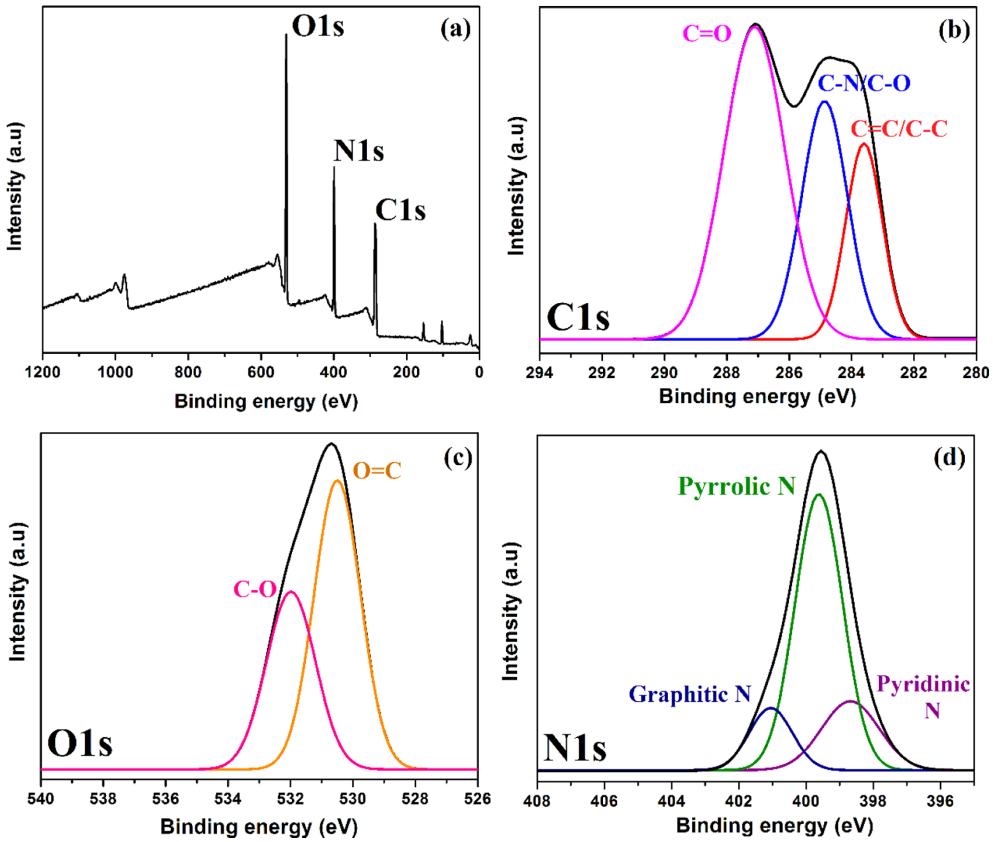

Fig. 3. (a) The XPS survey spectra of NDots. (b) High resolution XPS spectra of (b) C1s, (c) O1s and (d) N1s.

synthesis. The morphology of NDots was characterized by TEM image and shown in Figs. 1b and 1c. The size of NDots is 7-10 nm with spherical morphology.

As shown in Fig. 2, the optimal reaction temperature and time are 180 ℃ and 5h, respectively, which are used to synthesize all NDots used in this study. The aggregation of NDots at too high temperature or too long reaction time may decrease the PL emission intensity.

The chemical composition of NDots was investigated by XPS. The three strong peaks shown in XPS survey spectra (Fig. 3a) are originated from graphitic C1s (~284 eV), O1s (~532 eV) and N1s (~400 eV), which indicates that a huge amount of nitrogen atoms are incorporated in NDots. High resolution C1s and O1s spectra shown in Figs. 3b and 3c reveal that there are many oxygen related functional groups including carbonyl, hydroxyl, and carboxylic acids are present in NDots [32]. The high-resolution XPS N1s spectrum shown in Fig. 3d shows three peaks at 398.0-399.0, 400, and 401 eV which can be assigned to pyridinic, pyrrolic and graphitic nitrogen, respectively [33]. The abundant pyrrolic N indicates the high defect density in NDots fabricated in this study, which can result in strong and multicolor PL emission.

The functional groups of the NDots were analyzed by FTIR. As shown in Fig. 4, NDots show various functional groups. The peaks shown at 1505 and 3410 cm^{-1} can be attributed to the C=C stretching vibration and O-H stretching vibration. The other peaks shown at 892 and 1124, 1333, and 1411 cm^{-1} can be ascribed to N-H bond and

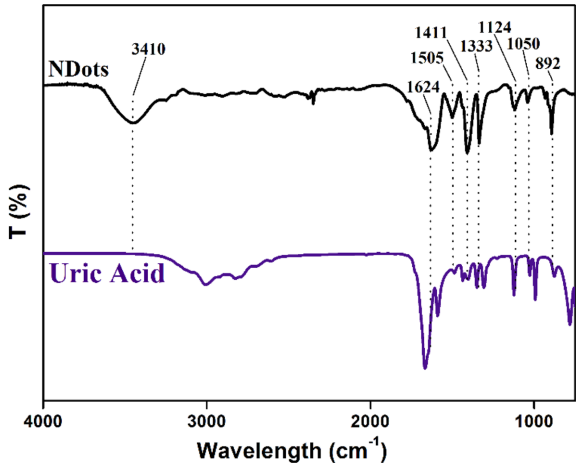

Fig. 4. FT-IR spectra of Uric Acid and the NDots.

ring vibration, the C-N bond vibration, and N-H bond vibration, respectively [34-38], which indicates a high nitrogen content in the NDots fabricated in this study.

The UV-Vis. absorption spectra are shown in Fig. 5a. The intense peak at 285 nm can be attributed to π–π* transitions of C=C and C=N groups [32] and the peak at 325 nm corresponds to n–π* transition of C=O groups on the surface of NDots [39]. Furthermore, the broad peak at 460 nm indicates the existence of aromatic structure of the NDots [40].

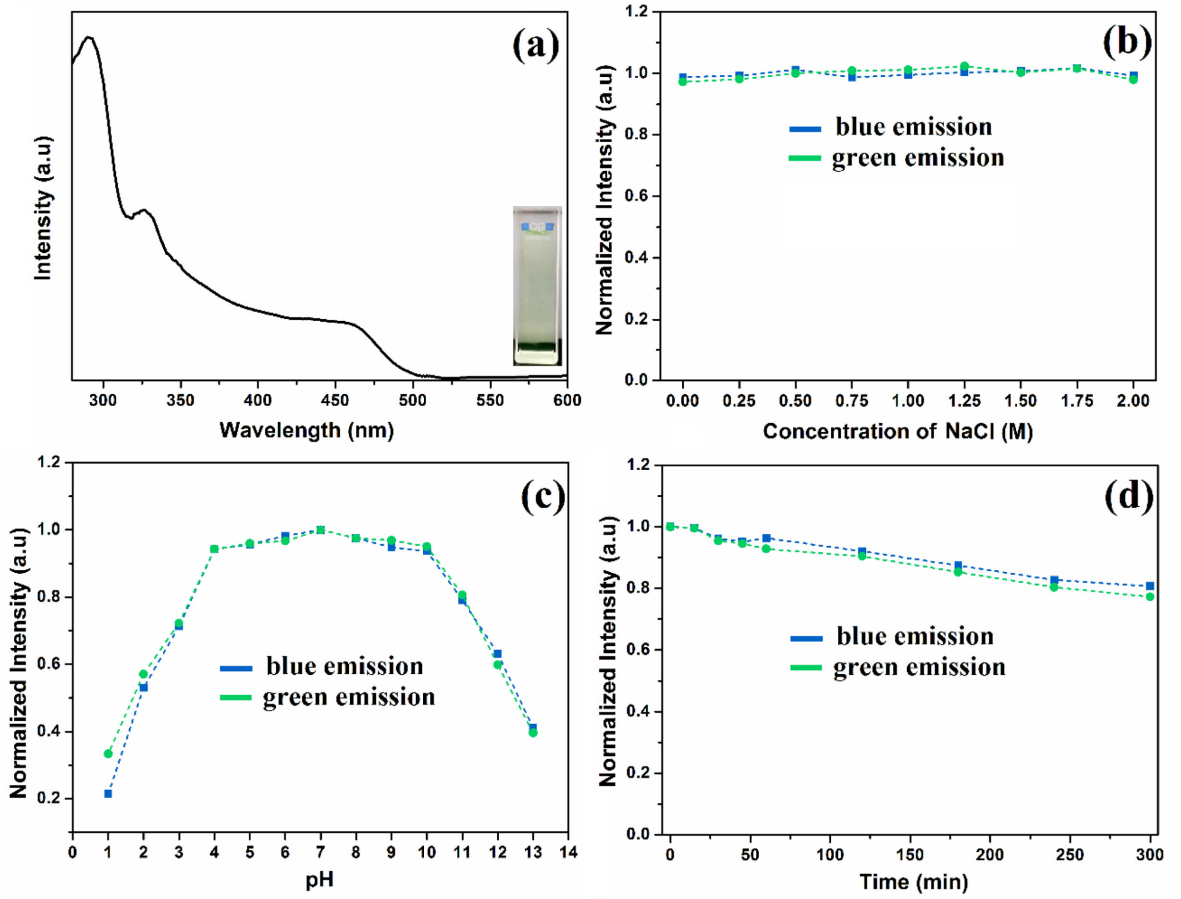

Fig. 5. (a) UV–vis absorption of the NDots and NDots in aqueous solution under white illumination (inset), (b) Effect of ionic strengths on the fluorescence intensity of NDots (controlled by various concentrations of NaCl), (c) Effect of pH on the fluorescence intensity of NDots and (d) dependence of fluorescence intensity on UV excitation time for NDots.

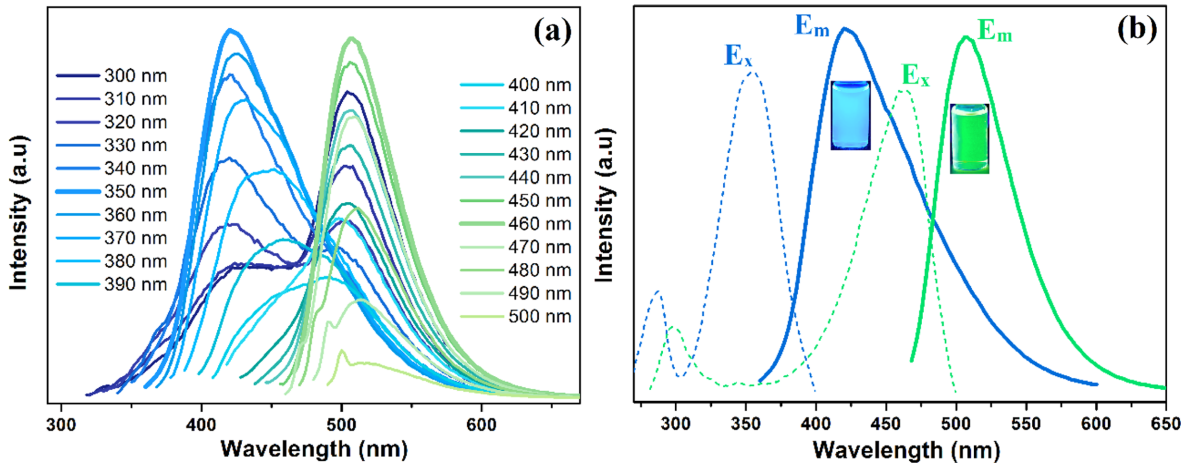

Fig. 6. The photoluminescence (PL) spectra of NDots: (a) recorded for progressively longer excitation wavelengths from 300 to 500 nm in a 10-nm increment; (b) the photoluminescence excitation and emission spectra of NDots in aqueous solutions (0.1 mg/mL), λ_{ex}= 350 nm with λ_{em}= 420 nm for blue color and λ_{ex}= 460 nm with λ_{em}= 510 nm for green color. Insets are corresponding photograph images.

The stability of NDots was investigated according to the ionic strength, pH of solution and the UV exposure are shown in Figs. 5b-d. The stable PL emission of NDots even at various ionic strength and wide pH range (4-10) indicates that NDots can work in the practical applications. In addition, the emission intensity is preserved up-to 80% to original value even after 5 h UV exposure, which indicates the excellent stability of NDots fabricated in this study.

The excitation wavelength-dependent emission behavior of the NDots was investigated by varying the excitation wavelengths from 300 to 500 nm. As shown in Fig. 6a, at low excitation wavelength

(300 to 330 nm) both a blue emission and green emission can be obtained. However, at medium (330 nm to 400 nm) and high excitation wavelength (400 nm to 500 nm), only the blue emission (~420 nm) and only the green emission (~510 nm) are observed. No fluorescent emission is recorded above 500 nm excitation wavelength. As shown in Fig. 6b, the bright dual fluorescence emission of the NDots in the visible region of the spectrum at different excitation wavelength is clearly observed by the naked eyes, which can be attributed to the abundant nitrogen atoms on the NDots surface. The origin of blue and green emission can be attributed to electron-hole recombination or intrinsic state emission, and the defect state emission, respectively.[41]

The quantum yields of NDots are 69% for the blue fluorescence emission and 61% for the green fluorescence emission, which are some of the highest values ever reported [18,27,29,32].

3-2. Ag^+ detection by NDots by the PL quenching

Various metal ions including Ag^+, Ca^{2+}, Co^{2+}, Cu^{2+}, Fe^{2+}, Fe^{3+}, Hg^{2+}, K^+, Mg^{2+}, Mn^{2+}, Na^+, Ni^{2+}, Pb^{2+}, Sn^{2+}, Zn^{2+} and Li^+ were added in the NDots solution (5 μg/mL, pH=7) and the sensitivity calculated by F_0-F/F_0 ($\Delta F/F_0$) of each sample, where F_0 is fluorescence intensity of pure NDots and F is that after metal ion addition.

As shown in Fig. 7, among all ions tested, NDots exhibits especially

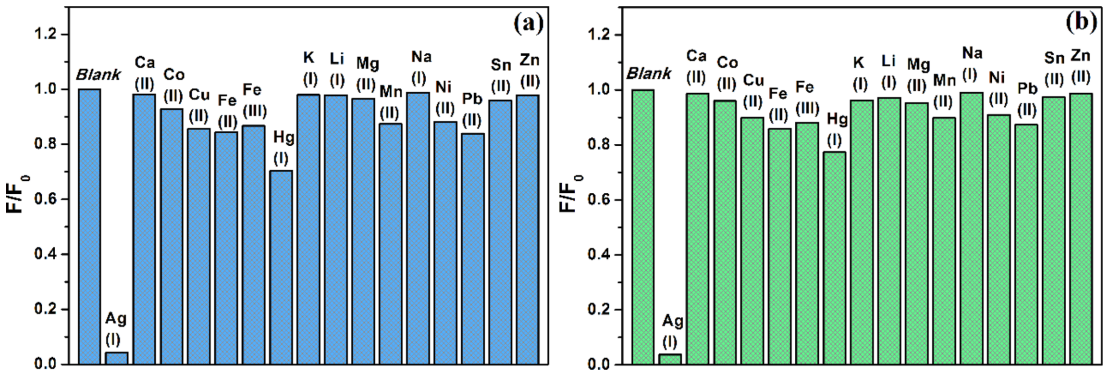

Fig. 7. F/F_0 value of aqueous N-CQDs solution in the presence of 500 μM of various metal ions at (a) λ_{ex}=350 nm and (b) λ_{ex}= 460 nm. F_0 and F correspond to the fluorescence intensity of NDots in the absence and presence of metal ions, respectively.

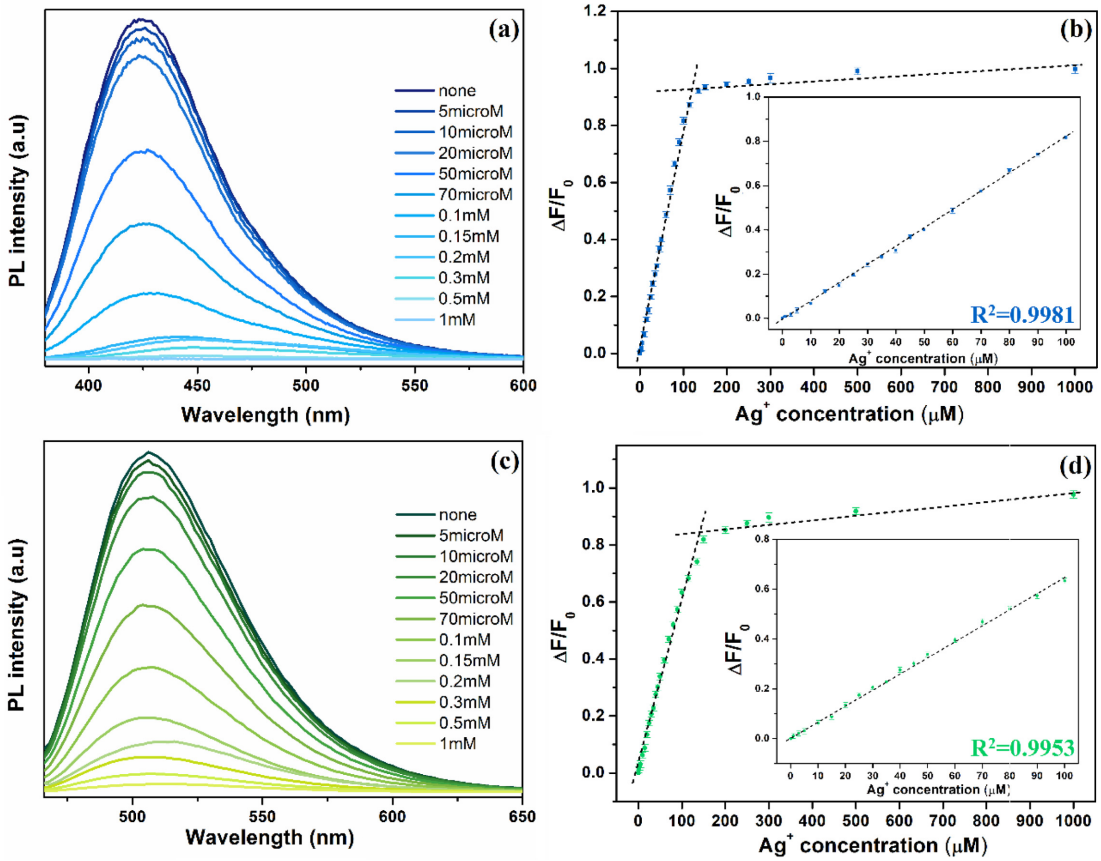

Fig. 8. (a) The PL spectra and (b) $\Delta F/F_0$ of the NDots in aqueous solution upon addition of various concentrations of Ag^+ (excitation wavelength = 350 nm). (c) The PL spectra and (d) $\Delta F/F_0$ of the NDots in aqueous solution upon addition of various concentrations of Ag^+ (excitation wavelength = 460 nm). Insets of (a) and (d): $\Delta F/F_0$ of the NDots at very low Ag^+ concentration (0~1 mM). F_0 and F correspond to the fluorescence intensities of NDots in the absence and presence of Ag^+ ions, respectively.

very high sensitivity towards Ag^+ ion, which can be due to the strong binding of Ag^+ ion on the surface of NDots [38]. Ag^+ ion acts as the soft acid while nitrogen atom (pyridinic N, pyrrolic N and graphitic N) acts as the soft base. When the conjugation of Ag^+–NDots complex is established, the release of recombination fluorescence decreases because of the inhibited the non-radiative electron and hole transfer [38]. Hg^{2+} ion can also restrain the radiative recombination of excitons, leading to fluorescence quenching [32,39]. In addition, a strong affinity of Hg^{2+} towards carboxylic, hydroxyl and amino groups on the surface of the NDots can be the reason for the relatively high fluorescence quenching of Hg^{2+} [32,39,42,43].

As shown in Fig. 8, NDots exhibit excellent sensitivity for Ag^+ at both excitation wavelengths of 350 and 460 nm. The linear range is 0 to 100 μM and the limits of detection (LODs) are 124 nM and 158 nM for blue emission and green emission, respectively. As compared in Table 1, NDots fabricated in this study exhibit one of the lowest LOD values ever reported values with a wide linear range.

To see the possibility of real applications, first, a precalculated amount of Ag^+ ions was dissolved in tap water and lake water that contains some amount of minerals. Then the concentration of Ag^+ ion was determined and compared with the precalculated values. As summarized in Table 2, the accuracy of the Ag^+ ion sensing by NDots for tap water and lake water is over 97%, which indicates the excellent sensitivity and selectivity of NDots fabricated in this study for the Ag^+ ion detection even for the real samples.

Table 2. The sensing accuracy of NDots for Ag^+ ion in the tab water and lake water

	Added Ag^+ (μM)	Measured Ag^+ (μM)	Accuracy (%)
Tap water	0	-	-
	5	4.981±0.173	99.62
	10	9.901±0.166	99.51
	50	49.75±0.21	99.50
	100	99.87±0.16	99.87
Lake water	0	-	-
	5	4.872±0.204	97.44
	10	9.864±0.186	98.64
	50	49.18±0.13	98.36
	100	97.63±0.29	97.63

3-3. The detection of EDTA by the Ag^+ ion saturated NDots

The quenched CDs can be regenerated by using proper chemicals, which can enable CDs sequential monitoring of multi chemicals by the "Turn-off" and "Turn-on" mechanisms [44,48-50]. As shown in Fig. 9a, significant enhancement of PL is observed especially when the EDTA is added to the Ag^+ saturated NDots, which can be attributed to the role of capping agent for Ag^+ ion. The EDTA, known as a metal chelator, can work as a clamped system to remove the Ag^+ ion by forming the cage-like structure around the Ag^+ ion [51].

The quicker recovery of green emission than that of blue emission can be due the position of PL emission. As the positions of green and blue emission are located at the surface and core of NDots, respectively,

Table 1. Comparison of the Ag^+ sensing properties of NDots with those of previous studies

Detection probe	Mechanism	Detection Limit (nM)	Linear Range (μM)	Reference
Amine-terminated GQDs	fluorescence quenching	3,060-9,270	-	[44]
Luminescent carbon nanoparticles	fluorescence quenching	386	-	[45]
Fluorescent CQDs hydrogels	fluorescence quenching	510	7-185	[46]
N-doped C-dots	fluorescence enhancement	1,000	1-100	[47]
N-doped GQDs	fluorescence quenching	168	0-40	[38]
NDots	fluorescence quenching	124 (Blue Emission) 158 (Green Emission)	0-100	this work

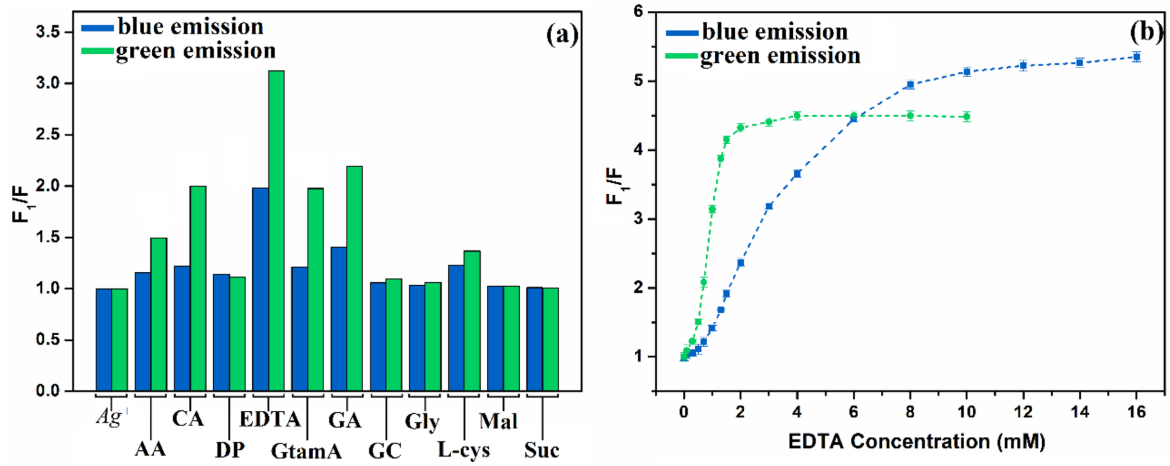

Fig. 9. (a) PL recovery (F_1/F) of Ag^+ saturated NDots after addition of various chemicals, where F and F^+ correspond to the fluorescence intensities of Ag^+ saturated NDots in the absence and presence of different species, respectively. (b) The PL recovery (F_1/F) of Ag^+ saturated NDots versus EDTA concentration. The excitation wavelengths of blue and green emissions are 350 and 460 nm, respectively.

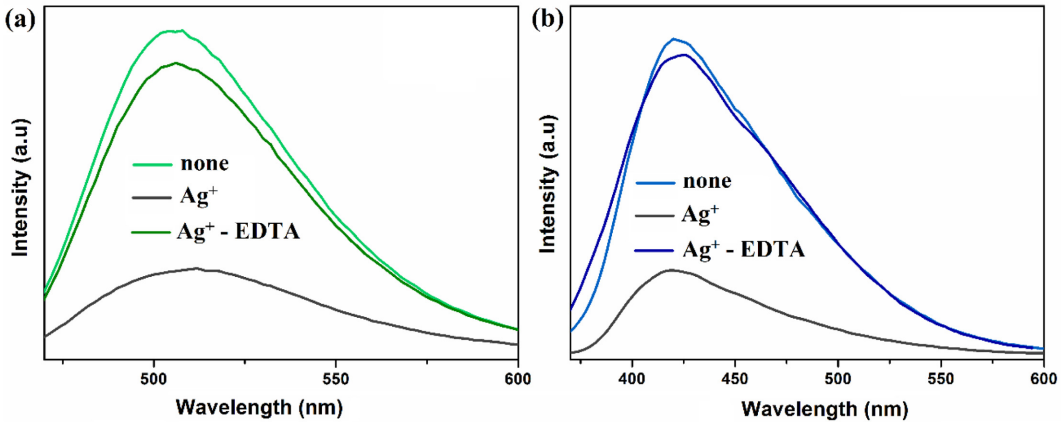

Fig. 10. The PL spectra of the NDots in aqueous solution upon addition of Ag^+ (0.1 mM) and EDTA (10 mM): (a) excitation at 350 nm and (b) excitation at 460 nm.

the green emission can be more easily recovered than that of blue emission by the EDTA. Therefore, low concentration of EDTA can be monitored by the green emission and high concentration by the blue emission, which makes Ag^+ saturated NDots wide detection range for the EDTA detection (Fig. 9b).

As shown in Fig. 10, the PL recovery of Ag^+ saturated NDots by the EDTA is as high as 93.04 and 87.12% for the green emission and blue emission, respectively.

4. Conclusions

Highly fluorescent NDots were synthesized using uric acid as a novel precursor by a facile, low-cost, ecofriendly and one-pot hydrothermal synthesis. The as-synthesized NDots exhibited blue and green dual emission with very high quantum yields of 69 and 61% for the blue and green emission, respectively. When the as-synthesized NDots were used as Ag^+ ion sensor, they exhibited a wide linear range of 0-100 μM and very low detection limit of 124 nM. In addition, Ag^+ saturated NDots can effectively monitor the EDTA level by the recovery of PL intensity.

Acknowledgment

This study was also supported by the National Research Foundation of Korea (NRF) grant funded by the Korea government (MSIT) (2022R1A2C1002901).

References

1. Hoa, L. T., Tien, H. N., Luan, V. H., Chung, J. S. and Hur, S. H., "Fabrication of a Novel 2D-graphene/2D-NiO Nanosheet-based Hybrid Nanostructure and Its Use in Highly Sensitive NO_2 Sensors," *Sens. Actuators B: Chem.*, **185**, 701-705(2013).
2. Hoa, L. T., Chung, J. S. and Hur, S. H., "A Highly Sensitive Enzyme-free Glucose Sensor Based on Co_3O_4 Nanoflowers and 3D Graphene Oxide Hydrogel Fabricated via Hydrothermal Synthesis," *Sens. Actuators B: Chem.*, **223**, 76-82(2016).
3. Choi, H., Ko, S. J., Choi, Y., Joo, P., Kim, T., Lee, B. R., Jung, J. W., Choi, H. J., Cha, M., Jeong, J. R., Hwang, I. W., Song, M. H., Kim, B. S. and Kim, J. Y., "Versatile Surface Plasmon Resonance of Carbon-dot-supported Silver Nanoparticles in Polymer Optoelectronic Devices," *Nat. Photon.*, **7**(9), 732-738(2013).
4. Li, X., Rui, M., Song, J., Shen, Z. and Zeng, H., "Carbon and Graphene Quantum Dots for Optoelectronic and Energy Devices: A Review," *Adv. Funct. Mater.*, **25**(31), 4929-4947(2015).
5. Li, H., He, X., Kang, Z., Huang, H., Liu, Y., Liu, J., Lian, S., Tsang, C. H. A., Yang, X. and Lee, S. T., "Water-Soluble Fluorescent Carbon Quantum Dots and Photocatalyst Design," *Angew. Chem. Int. Ed.*, **122**(26), 4532-4536(2010).
6. Martindale, B. C. M., Hutton, G. A. M., Caputo, C. A. and Reisner, E., "Solar Hydrogen Production Using Carbon Quantum Dots and a Molecular Nickel Catalyst," *J. Am. Chem. Soc.*, **137**(18), 6018-6025(2015).
7. Huang, Q., Zhang, H., Hu, S., Li, F., Weng, W., Chen, J., Wang, Q., He, Y., Zhang, W. and Bao, X., "A Sensitive and Reliable Dopamine Biosensor was Developed Based on the Au@carbon Dots–chitosan Composite Film," *Biosens. Bioelectron.*, **52**, 277-280(2014).
8. Cui, X., Zhu, L., Wu, J., Hou, Y., Wang, P., Wang, Z. and Yang, M., "A Fluorescent Biosensor Based on Carbon Dots-labeled Oligodeoxyribonucleotide and Graphene Oxide for Mercury (II) Detection," *Biosens. Bioelectron.*, **63**, 506-512(2015).
9. Luo, P. G., Sahu, S., Yang, S. T., Sonkar, S. K., Wang, J., Wang, H., LeCroy, G. E., Cao, L. and Sun, Y. P., "Carbon "quantum" Dots for Optical Bioimaging," *J. Mater. Chem. B*, **1**(16), 2116-2127(2013).
10. Zhu, S., Meng, Q., Wang, L., Zhang, J., Song, Y., Jin, H., Zhang, K., Sun, H., Wang, H. and Yang, B., "Highly Photoluminescent Carbon Dots for Multicolor Patterning, Sensors, and Bioimaging," *Angew. Chem. Int. Ed.*, **52**(14), 3953-3957(2013).
11. Guo, Y., Wang, Z., Shao, H. and Jiang, X., "Hydrothermal Synthesis of Highly Fluorescent Carbon Nanoparticles from Sodium Citrate and Their Use for the Detection of Mercury Ions," *Carbon*, **52**, 583-589(2013).
12. Liu, Y., Zhou, Q., Yuan, Y. and Wu, Y., "Hydrothermal Synthesis of Fluorescent Carbon Dots from Sodium Citrate and Polyacrylamide and Their Highly Selective Detection of Lead and

Pyrophosphate," *Carbon*, **115**, 550-560(2017).
13. Yang, Z. C., Wang, M., Yong, A. M., Wong, S. Y., Zhang, X.-H., Tan, H., Chang, A. Y., Li, X. and Wang, J., "Intrinsically Fluorescent Carbon Dots with Tunable Emission Derived from Hydrothermal Treatment of Glucose in the Presence of Monopotassium Phosphate," *Chem. Comm.*, **47**(42), 11615-11617(2011).
14. Wang, L., Zhu, S. J., Wang, H. Y., Qu, S. N., Zhang, Y. L., Zhang, J. H., Chen, Q. D., Xu, H. L., Han, W., Yang, B., Sun, H. B., "Common Origin of Green Luminescence in Carbon Nanodots and Graphene Quantum Dots," *ACS Nano*, **8**(3), 2541-2547(2014).
15. Hu, S., Huang, Q., Lin, Y., Wei, C., Zhang, H., Zhang, W., Guo, Z., Bao, X., Shi, J. and Hao, A., "Reduced Graphene Oxide-carbon Dots Composite as an Enhanced Material for Electrochemical Determination of Dopamine," *Electrochim. Acta*, **130**, 805-809(2014).
16. Song, Y., Zhu, S., Zhang, S., Fu, Y., Wang, L., Zhao, X. and Yang, B., "Investigation from Chemical Structure to Photoluminescent Mechanism: a Type of Carbon Dots from the Pyrolysis of Citric Acid and An Amine," *J. Mater. Chem. C*, **3**(23), 5976-5984(2015).
17. Zhou, M., Zhou, Z., Gong, A., Zhang, Y. and Li, Q., "Synthesis of Highly Photoluminescent Carbon Dots via Citric Acid and Tris for Iron(III) Ions Sensors and Bioimaging," *Talanta*, **143**, 107-113(2015).
18. Wang, L. and Zhou, H. S., "Green Synthesis of Luminescent Nitrogen-Doped Carbon Dots from Milk and Its Imaging Application," *Anal. Chem*., **86**(18), 8902-8905(2014).
19. De, B. and Karak, N., "A Green and Facile Approach for the Synthesis of Water Soluble Fluorescent Carbon Dots from Banana Juice," *RSC Adv*., **3**(22), 8286-8290(2013).
20. Mehta, V. N., Jha, S., Basu, H., Singhal, R. K. and Kailasa, S. K., "One-step Hydrothermal Approach to Fabricate Carbon Dots From Apple Juice for Imaging of Mycobacterium and Fungal Cells," *Sens. Actuators B: Chem*., **213**, 434-443(2015).
21. Sun, D., Ban, R., Zhang, P. H., Wu, G. H., Zhang, J. R. and Zhu, J. J., "Hair Fiber as a Precursor for Synthesizing of Sulfur- and Nitrogen-co-doped Carbon Dots with Tunable Luminescence Properties," *Carbon*, **64**, 424-434(2013).
22. Teng, X., Ma, C., Ge, C., Yan, M., Yang, J., Zhang, Y., Morais, P. C. and Bi, H., "Green Synthesis of Nitrogen-doped Carbon Dots From Konjac Flour with "off-on" Fluorescence by Fe^{3+} and l-lysine for Bioimaging," *J. Mater. Chem. B*, **2**(29), 4631-4639(2014).
23. Jiang, C., Wu, H., Song, X., Ma, X., Wang, J. and Tan, M., "Presence of Photoluminescent Carbon Dots in Nescafe® Original Instant Coffee: Applications to Bioimaging," *Talanta*, **127**, 68-74(2014).
24. Xu, Q., Pu, P., Zhao, J., Dong, C., Gao, C., Chen, Y., Chen, J., Liu, Y. and Zhou, H., "Preparation of Highly Photoluminescent Sulfur-doped Carbon Dots for Fe(iii) Detection," *J. Mater. Chem. A*, **3**(2), 542-546(2015).
25. Bourlinos, A. B., Trivizas, G., Karakassides, M. A., Baikousi, M., Kouloumpis, A., Gournis, D., Bakandritsos, A., Hola, K., Kozak, O., Zboril, R., Papagiannouli, I., Aloukos, P., Couris, S., "Green and Simple Route Toward Boron Doped Carbon Dots with Significantly Enhanced Non-linear Optical Properties," *Carbon*, **83**, 173-179(2015).
26. Wang, F., Hao, Q., Zhang, Y., Xu, Y. and Lei, W., "Fluorescence Quenchometric Method for Determination of Ferric Ion Using Boron-doped Carbon Dots," *Microchim. Acta*, **183**(1), 273-279(2016).
27. Edison, T. N. J. I., Atchudan, R., Shim, J. J., Kalimuthu, S., Ahn, B. C. and Lee, Y. R., "Turn-off Fluorescence Sensor for the Detection of Ferric Ion in Water Using Green Synthesized N-doped Carbon Dots and its Bio-imaging," *J. Photochem. Photobiol. B: Biol.*, **158**, 235-242(2016).
28. Wei, W., Xu, C., Wu, L., Wang, J., Ren, J. and Qu, X., "Non-Enzymatic-Browning-Reaction: A Versatile Route for Production of Nitrogen-Doped Carbon Dots with Tunable Multicolor Luminescent Display," *Sci. Rep.*, **4**, 3564(2014).
29. Yang, Z., Xu, M., Liu, Y., He, F., Gao, F., Su, Y., Wei, H. and Zhang, Y., "Nitrogen-doped, Carbon-rich, Highly Photoluminescent Carbon Dots from Ammonium Citrate," *Nanoscale*, **6**(3), 1890-1895(2014).
30. Yan, F., Zou, Y., Wang, M., Mu, X., Yang, N. and Chen, L., "Highly Photoluminescent Carbon Dots-based Fluorescent Chemosensors for Sensitive and Selective Detection of Mercury Ions and Application of Imaging in Living Cells," *Sens. Actuators B: Chem.*, **192**, 488-495(2014).
31. Hrbáč, J., Sichertová, D., Bancířová, M., Lasovský, J., Papadopoulos, K. and Nikokavouras, J., "Sensitized Chemiluminescence in Micellar Mixtures of Phthalhydrazide and Selected Dyes," *J. Photochem. Photobiol. A.*, **167**(2-3), 169-175(2004).
32. Zhang, R. and Chen, W., "Nitrogen-doped Carbon Quantum Dots: Facile Synthesis and Application as a "turn-off" Fluorescent Probe for Detection of Hg^{2+} Ions," *Biosens. Bioelectron*., **55**, 83-90(2014).
33. Sharifi, T., Nitze, F., Barzegar, H. R., Tai, C. W., Mazurkiewicz, M., Malolepszy, A., Stobinski, L. and Wågberg, T., "Nitrogen Doped Multi Walled Carbon Nanotubes Produced by CVD-correlating XPS and Raman Spectroscopy for the Study of Nitrogen Inclusion," *Carbon*, **50**(10), 3535-3541(2012).
34. Vasuki, G. and Selvaraju, R., "Growth and Characterization of Uric Acid Crystals," *Int. J. Sci. Res.*, **3**(8), 696-699(2014).
35. Xu, Y., Wu, M., Liu, Y., Feng, X. Z., Yin, X. B., He, X. W. and Zhang, Y. K., "Nitrogen-Doped Carbon Dots: A Facile and General Preparation Method, Photoluminescence Investigation, and Imaging Applications," *Chem. - Eur. J.*, **19**(7), 2276-2283(2013).
36. Dong, Y., Pang, H., Yang, H. B., Guo, C., Shao, J., Chi, Y., Li, C. M. and Yu, T., "Carbon-Based Dots Co-doped with Nitrogen and Sulfur for High Quantum Yield and Excitation-Independent Emission," *Angew. Chem. Int. Ed.*, **52**(30), 7800-7804(2013).
37. Wu, G., Feng, M. and Zhan, H., "Generation of Nitrogen-doped Photoluminescent Carbonaceous Nanodots via the Hydrothermal Treatment of Fish Scales for the Detection of Hypochlorite," *RSC Adv.*, **5**(55), 44636-44641(2015).
38. Tabaraki, R., Nateghi, A., "Nitrogen- Doped Graphene Quantum Dots: "Turn-off" Fluorescent Probe for Detection of Ag^{+} Ions," *J. Fluoresc.*, **26**(1), 297-305(2016).
39. Gao, Z., Lin, Z., Chen, X., Zhong, H. and Huang, Z., "A Fluorescent Probe Based on N-doped Carbon Dots for Highly Sensitive Detection of Hg^{2+} in Aqueous Solutions," *Anal. Methods* **8**(10), 2297-2304(2016).
40. Datta, K. K. R., Qi, G., Zboril, R. and Giannelis, E. P., "Yellow Emitting Carbon Dots with Superior Colloidal, Thermal, and Photochemical Stabilities," *J. Mater. Chem. C*, **4**(41), 9798-9803

(2016).
41. Zhu, S., Zhang, J., Tang, S., Qiao, C., Wang, L., Wang, H., Liu, X., Li, B., Li, Y., Yu, W., Wang, X., Sun, H. and Yang, B., "Surface Chemistry Routes to Modulate the Photoluminescence of Graphene Quantum Dots: From Fluorescence Mechanism to Up-Conversion Bioimaging Applications," *Adv. Funct. Mater.*, **22**(22), 4732-4740(2012).
42. Zhang, Y., Cui, P., Zhang, F., Feng, X., Wang, Y., Yang, Y. and Liu, X., "Fluorescent Probes for "off–on" Highly Sensitive Detection of Hg^{2+} and L-cysteine Based on Nitrogen-doped Carbon Dots," *Talanta*, **152**, 288-300(2016).
43. Gao, Z., Lin, Z., Chen, X., Lai, Z. and Huang, Z.-Y., "Carbon Dots-based Fluorescent Probe for Trace Hg^{2+} Detection in Water Sample," *Sens. and Actuators B: Chem.*, **222**, 965-971(2016).
44. Suryawanshi, A., Biswal, M., Mhamane, D., Gokhale, R., Patil, S., Guin, D. and Ogale, S., "Large Scale Synthesis of Graphene Quantum Dots (GQDs) from Waste Biomass and Their Use as an Efficient and Selective Photoluminescence on-off-on Probe for Ag^{+} Ions," *Nanoscale*, **6**(20), 11664-11670(2014).
45. Algarra, M., Campos, B. B., Radotic, K., Mutavdzic, D., Bandosz, T., Jimenez-Jimenez, J., Rodriguez-Castellon, E. and Esteves da Silva, J. C. G., "Luminescent Carbon Nanoparticles: Effects of Chemical Function Alization, and Evaluation of Ag^{+} Sensing Properties," *J. Mater. Chem. A*, **2**(22), 8342-8351(2014).
46. Cayuela, A., Soriano, M. L., Kennedy, S. R., Steed, J. W. and Valcárcel, M., "Fluorescent Carbon Quantum Dot Hydrogels for Direct Determination of Silver Ions," *Talanta*, **151**, 100-105(2016).
47. Qian, Z., Ma, J., Shan, X., Feng, H., Shao, L. and Chen, J., "Highly Luminescent N-Doped Carbon Quantum Dots as an Effective Multifunctional Fluorescence Sensing Platform," *Chem. - A Eur. J.*, **20**(8), 2254-2263(2014).
48. Zheng, M., Xie, Z., Qu, D., Li, D., Du, P., Jing, X. and Sun, Z., "On-Off-On Fluorescent Carbon Dot Nanosensor for Recognition of Chromium(VI) and Ascorbic Acid Based on the Inner Filter Effect," *ACS Appl. Mater. Interfaces*, **5**(24), 13242-13247(2013).
49. Huang, S., Qiu, H., Zhu, F., Lu, S. and Xiao, Q., "Graphene Quantum Dots as On-off-on Fluorescent Probes for Chromium (VI) and Ascorbic Acid," *Microchim. Acta* **182**(9), 1723-1731(2015).
50. Han, C., Wang, R., Wang, K., Xu, H., Sui, M., Li, J. and Xu, K., "Highly Fluorescent Carbon Dots as Selective and Sensitive "on-off-on" Probes for Iron(III) Ion and Apoferritin Detection and Imaging in Living Cells," *Biosen. Bioelectron.*, **83**, 229-236(2016).
51. Ajitha, B., Kumar Reddy, Y. A., Reddy, P. S., Jeon, H. J. and Ahn, C. W., "Role of Capping Agents in Controlling Silver Nanoparticles Size, Antibacterial Activity and Potential Application as Optical Hydrogen Peroxide Sensor," *RSC Adv.*, **6**(42), 36171-36179(2016).

Authors

Le Thuy Hoa: Postdoctoral Researcher, School of Chemical Engineering, University of Ulsan, Ulsan 44610, Korea; thuyhoakht@gmail.com

Jin Suk Chung: Professor, School of Chemical Engineering, University of Ulsan, Ulsan 44610, Korea; jschung@ulsan.ac.kr

Seung Hyun Hur: School of Chemical Engineering, University of Ulsan, Ulsan 44610, Korea; shhur@ulsan.ac.kr